研究論文

DOI: http://dx.doi.org/10.6108/KSPE.2013.17.3.037

Micro shock tube 유동에 대한 유한 격막 파막과정의 영향에 관한 수치 해석적 연구

Arun Kumar R* · 김희동**†

Numerical Simulation of the Effect of Finite Diaphragm Rupture Process on Micro Shock Tube Flows

Arun Kumar R* · Heuy Dong Kim**†

ABSTRACT

Recent years have witnessed the use of micro shock tube in various engineering applications like micro combustion, micro propulsion, particle delivery systems etc. The flow characteristics occurring in the micro shock tube shows a considerable deviation from that of well established conventional macro shock tube due to very low Reynolds number and high Knudsen number effects. Also the diaphragm rupture process, which is considered to be instantaneous process in many of the conventional shock tubes, will be crucial for micro shock tubes in determining the near diaphragm flow field and shock formation. In the present study, an axi-symmetric CFD method has been applied to simulate the micro shock tube, with Maxwell's slip velocity and temperature jump boundary conditions. The effects of finite diaphragm rupture process on the flow field and the shock formation was investigated, in detail. The results show that the shock strength attenuates rapidly as it propagates through micro shock tubes.

초 록

최근, micro shock tube는 Micro combustion, Micro propulsion, Particle delivery systems 등과 같은 다양한 공학응용분야에서 사용 되고 있다. Micro shock tube 에서 일어나는 유동 특성은 아주 작은 레이놀즈수 와 높은 누센수의 영향으로 인해 잘 알려진 기존의 macro shock tube 유동 특성과 상당한 차이가 나타난다. 또한 기존의 많은 shock tube의 순간적 과정으로 간주되는 격막파막 과정은 micro shock tube의 격막 근처의 유동장과 충격파 형성을 결정하는 중요한 요인이 될 것이다. 본 논문에서는 micro shock tube를 모사하기 위해 축 대칭, Maxwell's 슬립속도 조건과 온도 변화 경계 조건을 적용하여 수치 해석을 수행 하였다. 또한 유동장과 충격파 형성에 대한 유한 파막 과정의 영향을 자세히 조사 하였고, 결과로부터 충격파 강도는 micro shock tube를 통해 전파됨에 따라 급격히 감소하였다.

Key Words: Diaphragm Rupture(격막파막), Expansion Wave(팽창파), Micro Shock Tube(미소충격파관), Rarefaction(반사충격파), Unsteady Flow(비정상유동)

접수일 2012. 5. 22, 수정완료일 2013. 3. 11, 게재확정일 2013. 3. 14

* 학생회원, 안동대학교 기계공학과
** 종신회원, 안동대학교 기계공학과
† 교신저자, E-mail: kimhd@andong.ac.kr

[이 논문은 한국추진공학회 2012년도 춘계학술대회(2012. 5. 17-18, 금오공과대학교) 발표논문을 심사하여 수정·보완한 것임.]

1. Introduction

Micro shock tubes are recently employed in various micro devices such as micro heat

engines, micro propulsion, needleless injection devices etc. The functional details of a micro shock tube are similar to that of a conventional macro shock tube except its very small flow dimension. In general, a shock tube consists of a driver section at higher pressure and a driven section at relatively lower pressure, separated by a diaphragm. A sudden rupture of diaphragm causes rapid flow evolution from the driver to the driven section, which causes the formation of moving shock front. Due to the very small length scales, micro shock tube flow exhibits very low Reynolds number and relatively larger Knudsen number. As Knudsen number increases, the flow field is subjected to molecular effects which lead to rarefied flow conditions. This causes the near wall fluid to slip rather attaching to the wall.

Owing to these disparities in flow physics, the conventional macro shock tube understanding is not sufficient enough to predict the shock propagation and associated flow field for a micro shock tube.

Due to very small flow dimension micro shock tube exhibits very large surface area to volume ratio. This causes the boundary layer thickness and associated viscous losses to greatly influence the shock propagation. This has been observed by Duff[1] through his experimental studies on a small shock tube of 28.6 mm diameter. He also observed that the shock strength is much influenced by the initial pressure. Hence a lower initial pressure causes much attenuation of shock. Later Brouillette[2] devised a scaling factor for micro shock tube flows, which relates the diameter and initial pressure to the shock attenuation. Moreover as the initial operating pressure reduces the molecular mean free path increases and eventually increases the Knudsen Number (Kn), which is the ratio between the mean free path to flow diameter. Most of the micro shock tube flows, due to its inherent low diameter and low operating pressure, have a Knudsen number ranging between 0.01 to 0.1 which causes rarefaction effects and makes the near wall fluid to slip and an elevated temperature at the wall attached fluid. These properties alter the boundary layer effects and bring additional disparities to the shock flow field. A numerical study to investigate the shock propagation under slip condition was carried out by Zeitoun[3]. He also investigated molecular dynamics simulation[4] to improve the accuracy of shock propagation prediction in micro shock tubes, which becomes significant at flows having Kn greater than 0.1.

Most of the shock tube studies done in the past assumed an instantaneous diaphragm rupture process. But in actual scenario the diaphragm opens with a finite rupture time. This causes complex 2D flows near the diaphragm and a series of compression waves will be generated subsequent to finite opening steps and eventually will yield to shock waves. It is hard to derive some mathematical models to match the diaphragm opening process. Shigeru Matsuo[5] did an experimental analysis to determine the diaphragm rupture time at different low pressure ratios. They constructed the expansion head wave and expansion tail wave along the driver section. Because of a finite opening time these to loci will not meet at origin, which is the diaphragm position, but will produce an imaginary center downstream of the diaphragm for the non centered expansion wave and the gap between the loci of head and tail was considered to be the diaphragm opening time. The experimental setup details are shown in Fig. 1.

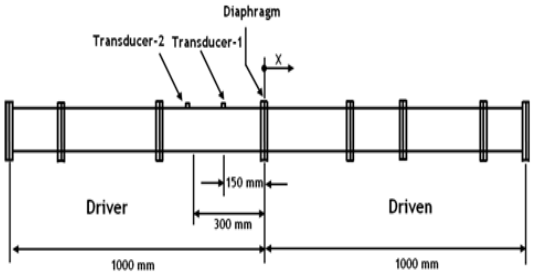

Fig. 1 Schematic diagram for the experimental setup

The phenomenon of diaphragm rupture is a highly complicated three-dimensional process. In the above experimental work the authors suggested a quadratic function to imitate the diaphragm rupture process. Another model which uses a cosine function for the diaphragm opening area with respect to opening time was proposed by Outa[6].

In the past there have been some studies to understand the effect of diaphragm rupture process on macro shock tubes[7, 8, 9]. But in the case of micro shock tubes the unsteady shock evolution and the associated flow field with a finite diaphragm rupture process is even more complicated due to the slip and boundary layer effects. In the present study a 2D axi-symmetric CFD approach was used to simulate the unsteady flow evolution and shock propagation inside a micro shock tube considering the diaphragm rupture process.

2. Numerical Simulation

For the present study an axi-symmetric shock tube model of 1 mm diameter was considered as shown below.

The determination of diaphragm rupture time for a micro shock tube is extremely hard due to very small rupture time scale and experimental difficulties due to very small

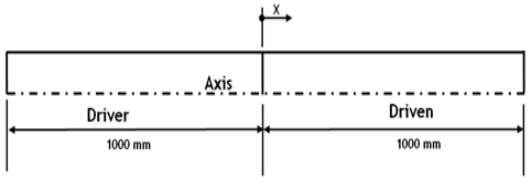

Fig. 2 Schematic diagram for micro shock tube (ϕ1 mm)

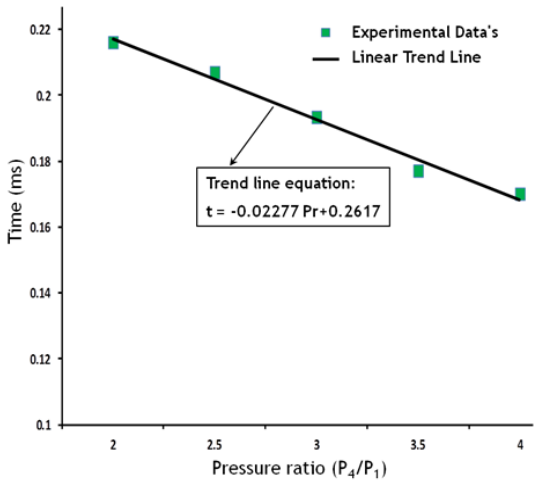

Fig. 3 Experimental diaphragm opening time at various pressure ratios

flow dimensions. Few years back, Shigeru Matsuo experimentally found out the diaphragm rupture time for a macro shock tube of 65.5 mm diameter under various low pressure ratios as discussed in the above section and the experimental diaphragm opening results are shown in Fig. 3.

From this experimental result of conventional macro shock tube the diaphragm rupture time for a micro shock tube of 1 mm diameter and at low initial pressure can be found by using some interpolation techniques as explained below.

The diaphragm rupture time mainly depends on three factors:

1. Diaphragm area,
2. Net pressure (P_4-P_1) acting across the

diaphragm

3. Diaphragm thickness

The experimental result (Fig. 3) at the minimum pressure ratio (P_r=2; P_4=101300 Pa; P_1=50650 Pa) gives a rupture time of 0.216 ms. The net rupture force for this case will be 50650 Pa. But for studying the slip effects on shock propagation the numerical study should be carried out at a much lower operational pressure. It can be noted that the same net pressure can be obtained at a much lower initial pressures (P_4=51161 Pa; P_1=511.61 Pa) but with a higher pressure ratio of 100. For the latter case also the diaphragm rupture time will be 0.216 ms since the diaphragm area, net pressure force and diaphragm thickness remained unaltered. But this low pressure produces a Knudsen number of 0.01 at the driven section, which is in the verge of no slip wall conditions and hence not suitable for studying the rarefaction effect on shock propagation.

From the above experimental results it can be observed that the diaphragm rupture time shows linear trend, as t = -0.02277 P_r+0.2617, with respect to pressure ratio. It can also be noted that a lower pressure ratio yields a low net pressure force in which case a much lower initial operating pressure can be considered. For this purpose opening time at a pressure ratio of 1.4 was found based on the linear trend. The net force acting across the diaphragm for this case (P_r=1.4; P_4=101300; P_1=72357 Pa) will be 28942 Pa. The same net pressure force can be achieved with a lower driver and driven pressure of 29235 Pa and 292.35 Pa respectively but with a higher pressure ratio of 100. The very low pressure in the driven tube makes the Knudsen number to 0.025 and the flow will fall under slip conditions. The diaphragm opening time based on the linear trend line equation will be 0.2296 ms. This time is for shock tube of 65.5 mm diameter. Assuming a direct relationship of diaphragm rupture time with area, the rupture time for a 1 mm tube can be easily found out and is about 0.053 μs.

The total diaphragm opening time was divided into 30 discrete time steps and the diaphragm opening radius at each time step is found based on some assumed opening functions with respect to time as shown in below equations.

Linear Opening :

$$r = 9.931 \times t \tag{1}$$

Cosine Opening (by Outa[6]) :

$$\frac{d^2}{D^2} = 1 - \cos\left(\frac{\pi}{2}\left(\frac{t - t_r}{T}\right)^2\right) \tag{2}$$

Quadratic Opening (Matsuo[5]) :

$$t = \left(\left(\frac{r}{R}\right)^2 T\right) \tag{3}$$

In the above equations r represents the opening radius at some arbitrary time t. R represents the initial radius of the diaphragm and T represents the total diaphragm opening time.

The diaphragm was also divided into 30 segments. At the starting of the simulation, all the segments were considered as wall and subsequent to each time step the segments were sequentially opened. Each segment opening results in the corresponding opening radius at that time. Thus the entire diaphragm rupture process was replicated using a thirty discrete step process. Table 1 shows three different cases considered for the present simulation with different opening radius functions.

Table 1. Initial conditions for different opening functions

Cases	Dia	P_4/P_1	P_1 (Pa)	Opening Function
1	1 mm	100	292.35	Linear
2	1 mm	100	292.35	Cosine
3	1 mm	100	292.35	Quadratic

Different opening process has been shown in Fig. 4. In the present study the actual continuous opening process has been replaced by discrete step opening process. As sufficient number of opening steps (30 steps) has been considered the piecewise step function will nearly match the continuous function.

The flow physics was mathematically modeled using unsteady Reynolds Averaged Navier-Stokes equations. SST k-ω model was used to predict the turbulent eddies. Ideal gas behavior was considered for all the species and viscosity variation with respect to temperature was modeled using Sutherland viscosity model. The flux component of the governing equation was discretized using AUSM scheme. A second order implicit scheme was used for the temporal discretization. The extrapolation of cell centre values to the face centers was done using third order MUSCL schemes. The governing flow equations were solved in a coupled manner using commercial solver, Fluent. To account for the rarefaction effects which happen at low pressure Maxwell's slip velocity and temperature jump equations[10], as shown below, were employed. User defined functions[11] were used to input these equations to the solver and subsequent to each flow iteration the pre defined functions for slip conditions were called into the solver and executed to update the near wall fluid velocity and temperature.

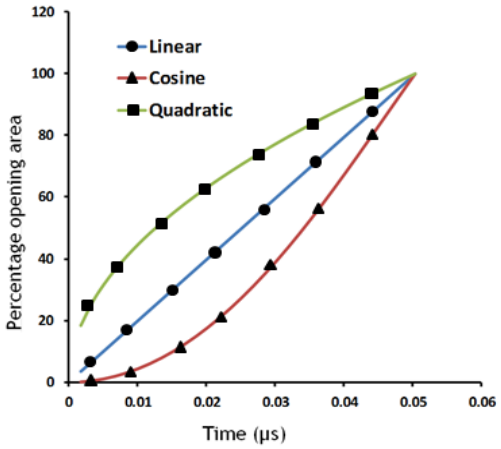

Fig. 4 Diaphragm opening area variation with respect to time based on different opening functions

$$U_w - U_g = \left(\frac{2-a_v}{a_v}\right)\frac{\lambda}{\delta}(U_g - U_c) \tag{4}$$

$$T_s - T_w = 2\left(\frac{2-a_T}{a_T}\right)\frac{\lambda}{\delta}(U_g - U_c) \tag{5}$$

$$\lambda = \frac{k_B T}{\sqrt{2}\,\pi\sigma^2 p} \tag{6}$$

Here the subscript g, c and w refer to gas, cell centre and wall quantities respectively. a_v and a_t are the momentum and thermal accommodation coefficients respectively. λ is the molecular mean free path.

2.1 Validation

The accuracy of different diaphragm opening functions was compared with the experimental results of Matsuo. In the experiment the expansion wave propagation has been monitored at 150 mm behind the diaphragm.

Figure 5 shows the pressure value at the measuring point at various times. It can be clearly noted that the quadratic function shows more closer results compared with the experimental values. The cosine opening

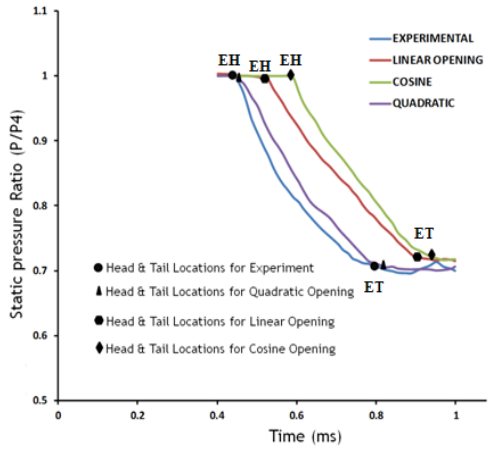

Fig. 5 Static pressure comparisons in the driver section for different cases at X/D=-2.29

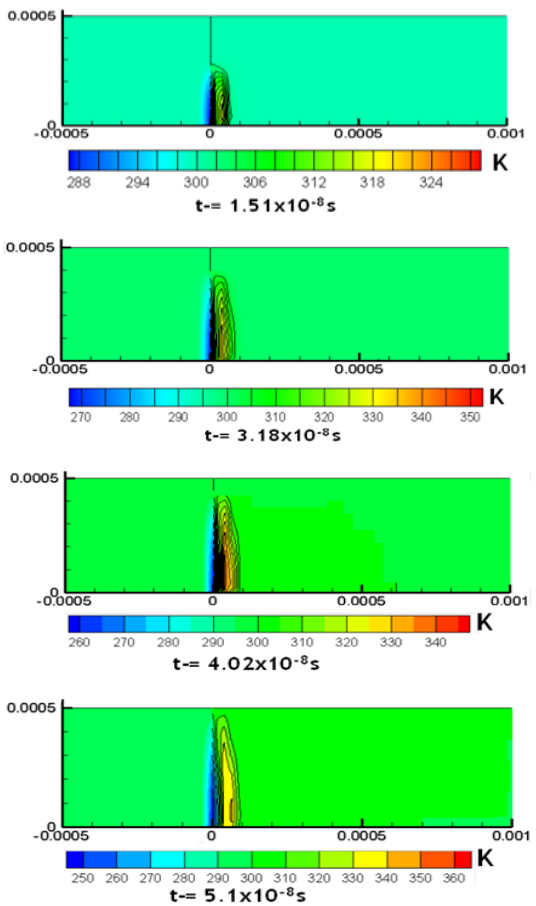

Fig. 6 Static temperature distributions in the driven section at different diaphragm opening stages

function shows a considerable deviation from the experimental values and this may be due to the fact that for the cosine opening the initial rupture process is gradual and then it becomes rapid. Because of this the flow evolution takes more time for cosine opening process were as for quadratic opening function the opening area grows rapidly at the beginning and then slows down.

3. Results and Discussion

As the diaphragm starts to open the high pressure fluid from the driver section escapes into the low pressure driven section. This results in a series of compression waves that eventually gets piled up and leads to a shock wave. So the shock front will be generated after a particular distance ahead of the diaphragm. The static temperature contours at various times for a quadratic opening process as shown in Fig. 6 clearly explains this.

Figure 7 shows expansion head, contact and shock wave propagation inside the micro shock tube. The contact location was identified as the location where a sudden rise in temperature happens and shock position is the location where the temperature suddenly dips.

The ideal viscous shock tube equation explains that the shock strength will be a constant value. But in real situation this may not be the case due to viscous losses, finite diaphragm rupture process and turbulent losses. Because of the gradual opening consideration, a fully developed flow into the driven section takes some time. Due to this factor, the shock front will be generated after some particular distance ahead of the diaphragm where as for a sudden rupture case an instantaneous production of shock

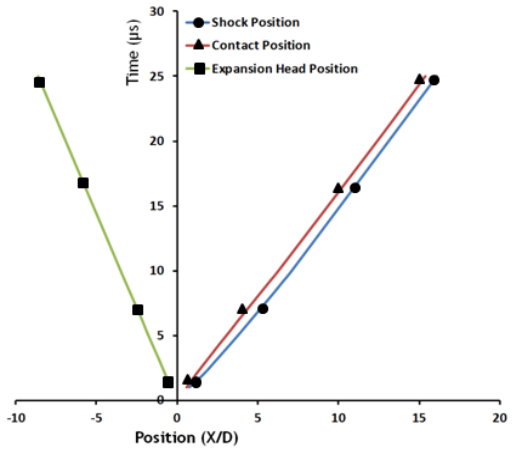

Fig. 7 Expansion, Contact and Shock wave propagation (x-t diagram) distances at various times

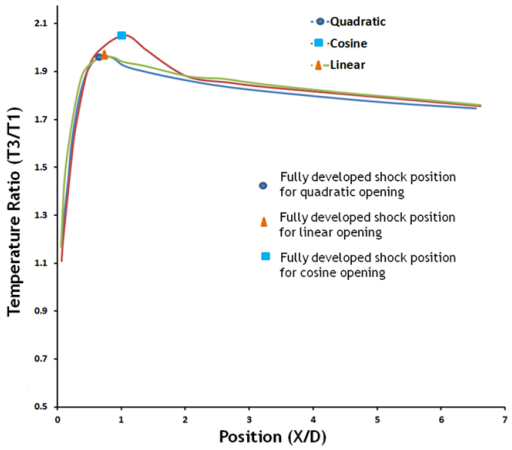

Fig. 8 Temperature ratio distributions across the shock front along the axis under different opening conditions

front can be visualized. So for real situation the shock strength initially increases and then decreases. The temperature ratio across the shock is a direct indication for the shock strength and this is being compared along the length as shown in Fig. 8.

The fully developed shock position was determined as the location where the shock strength reaches its maximum value. It can be observed from Fig. 8 that a fully developed shock front in the case of a cosine diaphragm opening function occurs at a larger distance from the diaphragm as compared with that of a quadratic opening. This can be attributed due to the fact that for quadratic function the opening process is much rapid in the beginning and then becomes gradual where as in the case of cosine opening this is just reverse process. The rapid opening of diaphragm at the beginning causes a much faster development of flow evolution there by producing a completely developed shock front at a much advanced distance compared with that of cosine opening model. Also the flow losses happening at the beginning will be higher for the case of quadratic opening process due to a higher flow rate and this result in a lesser temperature rise downstream of the shock for this case compared with the cosine opening case. The shock development distance for different opening functions is shown in Table 2.

Table 2. Shock development distance from diaphragm for various opening functions

Opening Function	Shock Formation distance from diaphragm
Linear	0.88 mm
Cosine	1.06 mm
Quadratic	0.74 mm

The shock propagation inside micro shock tube suffers much more attenuation in shock strength compared to macro shock tube flows. This is mainly because boundary layer thickness fills much of the core flow and produces more viscous losses. If the initial operating pressure is low then rarefaction effects happens and this changes the near wall flow field. This eventually alters the shock propagation phenomenon. At low pressure the

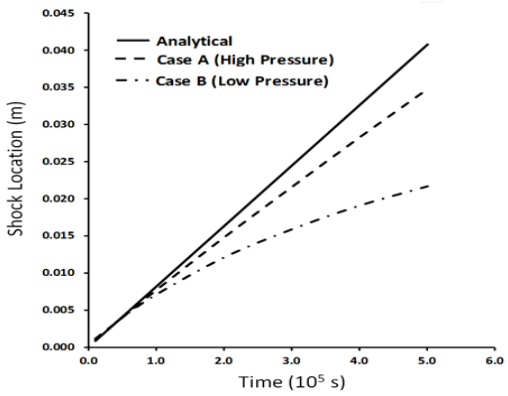

Fig. 9 Shock location along axis (d=2 mm) at different initial pressure conditions

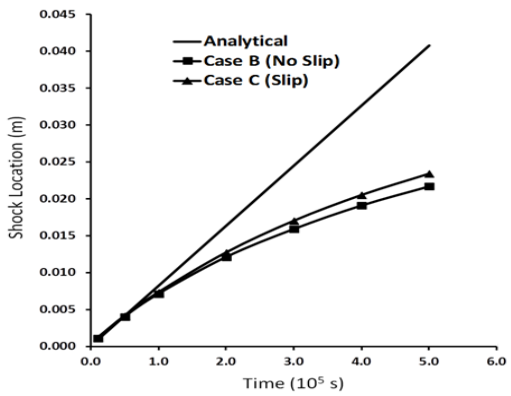

Fig. 10 Shock location along axis (d=2 mm) for slip and no slip case

Table 3. Initial conditions for studying the pressure dependency and slip effects on shock propagation

Cases	P_4/P_1	P_1 (Pa)	Dia (mm)	Wall Conditions	Diaphragm Opening
A	15	500	2	No Slip	Sudden Rupture
B	15	50	2	No Slip	Sudden Rupture
C	15	50	2	Slip	Sudden Rupture

Table 4. Initial conditions for studying the diameter dependency on shock propagation

Cases	P_4/P_1	P_1 (Pa)	Dia (mm)	Wall Conditions	Diaphragm Opening
1	15	50	2	Slip	Sudden Rupture
2	15	50	1	Slip	Sudden Rupture
3	15	50	0.5	Slip	Sudden Rupture

boundary layer thickness increases and this also leads to much attenuation compared to a high operating pressure system. Five CFD simulations with sudden rupture conditions were carried out to simulate the effect of initial pressure and diameter on micro shock tube flows, as shown in the Table 3.

The shock propagation distance along the distance as shown in Fig. 9 clearly explains the attenuation phenomenon. It can be clearly noticed that the shock location for micro shock tube (Case A) clearly drags from the ideal analytical position. At low pressure (Case B) the attenuation effect will be more due to the larger boundary layer thickness produced. The consideration slip conditions (Case-C) introduces additional velocity and temperature jump to the wall attached fluid. This produces more pronounced core flow in the case of slip case flow and reduces the attenuation which can be observed from Fig. 10.

Three cases with different diameters as shown in Table 4, are simulated to investigate the effect of diameter on shock propagation.

As the tube diameter decreases the shock propagation distance suffers more drastic attenuation. This is because, the reduction in tube diameter causes the boundary layer flow to fill majority of the core flow volume and elevates the losses. This attenuation effects can

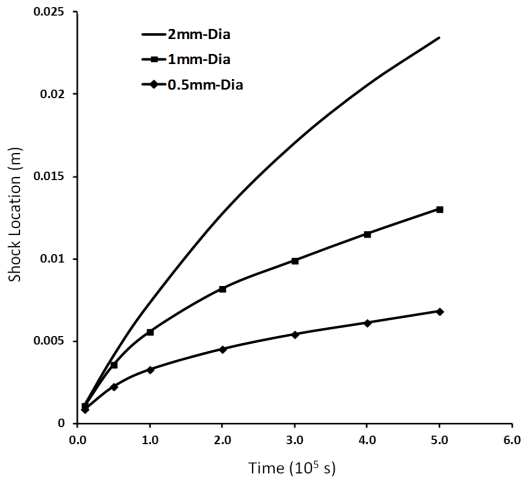

Fig. 11 Shock locations along axis for different tube diameters

be clearly observed from the shock propagation distance along the axis for different diameter cases as shown in Fig. 11.

4. Conclusions

In the present study the effect of diaphragm opening process on the shock evolution with three different opening functions (linear, cosine and quadratic functions) were numerically studied. The consideration of finite rupture time results in the development of fully developed shock front at certain distance ahead of the diaphragm. The shock development distance is minimum in the case of a quadratic opening function. The opening process will be rapid at the initial stages for quadratic opening function compared to other opening process and hence flow evolution will be faster for this case which results in less shock development distance. The shock strength initially increases to reach a maximum value and then decreases. This is because during the gradual opening process the flow evolution into the driven tube initially accelerates to a maximum point after which the flow viscous resistance dampens the shock Mach number. The shock propagation attenuates in the case of a micro shock tube compared to a macro shock tube. This is mainly because of the severe viscous losses associated with the boundary layer thickness which will considerably affects the core flow due to very small flow diameter. As the driven section pressure reduces a thicker boundary layer forms compared to the high pressure case. This produces more loss in low pressure case and subsequently produces more attenuation to shock movement. The implementation of slip boundary condition on the walls to simulate the rarefaction effects reduces the losses produced and this eventually helps in shock propagation.

Acknowledgement

This work was supported by the National Research Foundation of Korea (NRF) grant funded by the Korea government (MEST) (2011-0017506)

References

1. Duff, R. E., "Shock Tube performance at initial low pressure," Physics of Fluids, Vol. 4, 1958, pp.207-216
2. Brouillette, M., "Shock waves at microscales," Shock Wave, Vol. 13, 2003, pp.3-12
3. Zeitoun, D. E. and Burtschell, Yves., "Navier-Stokes computations in micro shock tubes," Shock Waves, Vol. 15, 2006, pp.241-246

4. Zeitoun, D. E., Burtschell, Yves., Graur, I. A., Ivanov, M. S., Kudryavtsev, A. N., and Bondar, Y. A., "Numerical simulation of shock wave propagation in micro channels using continuum and kinetic approaches," Shock Waves, Vol. 19, 2009, pp.307-316
5. Shigeru, M., Mamun, M., Nakano, S., Srtoguchi, T., and Kim, H. D., "Effect of a diaphragm rupture process on flow characteristics in a shock tube using dry cellophane," International Conference on Mechanical Engineering, 2007
6. Outa, E., Tajima, K., and Hayakawa, K., "Shock tube flow influenced by diaphragm opening (two-dimensional flow near the diaphragm)," 10th International Symposium on shock waves and Shock Tubes, 1975
7. Rothkopf, E. M. and Low, W., "Diaphragm opening process in shock tubes," Physics of Fluids, Vol. 17, Issue 6, 1974, pp.1169-1173
8. Mizoguchi, E. M. and Aso, S., "The effect of diaphragm opening time on the feasibility of tuned operation in free piston shock tunnels," Shock Waves, Vol. 19, 2009, pp.337-347
9. Roy, S. H., Larry, C. F., and James, B. K., "Behavior of burst diaphragm in shock tubes," Physics of Fluids, Vol. 18, Issue 10, 1975, pp.1249-1152
10. Karniadakis, G. E. M. and Beskok, A., Micro Flows fundamentals and Simulation, Springer, Berlin Heidelberg New York, 2000
11. Fluent user's guide manual, http://www.fluent.com/